INTERNATIONAL JOURNAL OF AUTOMOTIVE AND MECHANICAL ENGINEERING
ISSN: 2229-8649 e-ISSN: 2180-1606
VOL. 21, ISSUE 1, 2024, 11139 – 11154
DOI: https://doi.org/10.15282/ijame.21.1.2024.15.0861

RESEARCH ARTICLE

Simulation of the Performance of an Electrically Turbocharged Engine Over an Urban Driving Cycle

Kamalleswaran Subramaniam[1]* and Wan Saiful-Islam Wan Salim[2]

[1]Faculty of Mechanical & Manufacturing Engineering, Universiti Tun Hussein Onn Malaysia, 86400 Parit Raja, Johor, Malaysia
[2]Centre for Energy and Industrial Environment Studies (CEIES), Universiti Tun Hussein Onn Malaysia, 86400 Parit Raja, Johor, Malaysia

ABSTRACT - The study aimed to estimate the energy recovery potential of a decoupled electric turbocharger and its boosting ability in a spark-ignition engine using simulation-based work. Passenger vehicle engines operate at low loads and speeds, requiring characterization and estimation of energy available for recovery under normal driving conditions. A 1-D numerical model of the engine and boosting system was developed to predict energy recovery over steady-state full-load operating conditions, part-load conditions, and actual, transient Klang Valley and Kuala Lumpur drive cycle conditions. The electric turbocharged engine consists of two motors and a battery pack, which were modeled and utilized using GT-Power engine simulation software. The study found that the electrical turbocharger system could recover 0.57 kW and 0.50 kW at 2500 rpm and 3000 rpm, respectively. Part-load studies showed that the maximum amount of electrical energy recovered at 6500 rpm was 5.25 kW. Drive cycle analysis revealed that fuel consumption was the same for both engine models due to the similar turbocharger output performance and lower back pressure caused by the recalibrated wastegate controller. This was partially mitigated by the inclusion of two electric motors. Drive cycle analysis revealed that the electric turbocharger can perform better than a conventional turbocharger when optimized.

ARTICLE HISTORY
Received : 10th May 2023
Revised : 26th Jan. 2024
Accepted : 11th Feb. 2024
Published : 20th Mar. 2024

KEYWORDS
Electric turbocharger
1-D simulation
Energy recovery
Boosting system

1.0 INTRODUCTION

A significant contributor to the greenhouse gases that contribute to global climate change is the automotive industry. The automotive sector has been subject to significant laws as a result, which are intended to lessen and eliminate the harmful effects on the environment. Under Euro 6 regulations, carbon monoxide (CO) and nitrogen oxide (NOx) emissions are limited to 1g/km and 0.08 g/km, respectively, while carbon dioxide (CO2) emissions are limited to 98 g/km [1]. Downsizing using turbochargers is one of the methods that has gained popularity because of this. Inefficient operation at low engine speeds is one of the most frequent problems with smaller engines. Salim *et al.* [2] conducted research to establish the advantages of stop-start, cylinder deactivation (CDA), and engine downsizing technologies in relation to fuel economy. The result was that the fuel consumption worsened on the downsized turbocharged engine by 7.5%. The drivability of the car suffers because of the poor transient response frequently associated with turbocharged engines, even though the advantages of the turbocharged engine make it a popular choice for auto manufacturers to comply with emission laws. The option of recovering the exhaust gases lost through the wastegate is made possible by the installation of an electronic turbocharger, which also reduces the delay in transient reaction. To address the disadvantages of traditional turbochargers, electric or hybrid turbochargers are currently being introduced into the hybrid car sector.

Waste heat recovery has been a common approach for engine builders to boost the volumetric efficiency of their engines. Alias *et al.* [3] assessed the waste heat recovery systems' downsizing technology. A Caterpillar researcher's design by Hoppman and Algrain, an electric turbo-compounding system that was examined, placed the motor between the turbine and compressor [3]. Traditional turbochargers employ wastegates to bypass the turbine exhaust gases, which means they are not fully using the boosting system's capability for energy recovery [4]. The functioning parameters of an internal combustion engine with a hybrid turbocharger were attempted to be analyzed by Gruji *et al.* [5]. The result was that using a hybrid turbocharger improved engine economy and performance. Research on the function of turbogenerators in energy recovery systems was conducted by Nicolay *et al.* [6]. When recovery systems to boost engine efficiency were implemented, it was discovered that the thermal efficiency of the engine increased by 10-12%.

Research on the effectiveness of three distinct kinds of electric turbochargers was conducted by Wei *et al.* [7]. An electrically assisted turbocharger produced a lot of electrical power while the system was under high load, but none when it was under low load, which had no impact on fuel efficiency. With the performance of electric forced induction in mind, Woongkul *et al.* [8] investigated different electric turbocharger compounding, electric turbocharger configurations, high-speed machines, power electronics, and control systems. The researchers outlined the benefits and drawbacks of the electric forced induction technology now in use. In research by Pinto *et al.* [9], the number of shafts and electric efficiency-enhancing components were evaluated in relation to various gas microturbine topologies derived from automotive turbochargers. The best-performing setup, according to the researchers, had a single turbocharger, a single turbo

*CORRESPONDING AUTHOR | S. Kamalleswaran | ✉ kamalles.95@gmail.com

compound component, an intercooler, a heat recovery device, and a two-stage reheating mechanism. According to Mamdouh *et al.* [10], each electric turbocharger architecture was examined for a specific purpose, hence none of the designs could be deemed superior to another configuration.

Exergy energy availability studies were also done to determine the energy recovery potential of the system. The exergy availability and losses between the Organic Rankine Cycle (ORC) and Electric Turbo-Compounding (ETC) were compared by Muhammad *et al.* [11]. The ORC had a higher exergy capacity compared to the ETC but was shorthanded by the huge exergy losses, which were minimal in the ETC. Imran *et al.* research's [12] also concentrated on the energy that may be obtained from the exhaust manifold. According to this study, even at engine speeds as low as 2200 rpm, energy may be recovered.

Removal of the wastegate valve was also a perspective researcher investigated concerning the electric turbochargers. The potential use of electric turbochargers to manage load and determine if they can take over the role of a wastegate valve was examined by Pavlos *et al.* [13]. The research included a comprehensive numerical analysis of the possibility of e-turbocharging to manage load and, if feasible, play the role of the wastegate valve. The wastegate can be made redundant by employing a bigger turbine, however doing so makes the engine respond slower and uses more energy at low engine speeds. The maximum power output decreases by 5% but efficiency and energy generation over the whole engine range are boosted by employing a 10% smaller turbine and a 20% higher pre-turbine pressure. The effects of intake e-boosting on the performance of gasoline compression ignition engines running at 2000 rpm were investigated by Liu *et al.* [14]. It was discovered that e-boosting at the intake manifold significantly raises the IMEP and system effectiveness.

Numerous academics have conducted studies on the effects of varying motor power levels on BSFC and fuel consumption. First, it was important to confirm that there had been prior research on electric motors that could provide power at the high speeds that turbochargers typically run at, which are between 100,000 and 200,000 rpm. The investigation conducted by Adrien *et al.* [15] using a high-speed permanent magnet synchronous motor to produce 4 kW of power at a maximum operating speed of 150,000 rpm confirmed this working speed of the motor. High-speed electric motors were used to show the utilization of turbocharger applications by El-Shahat *et al.* [16]. One method prioritized optimization, while another was cost-effective. A 1-D simulation model with electrically assisted turbochargers was created by Mamdouh *et al.* [17] and intended to be utilized in the development of a centrifugal turbocharger compressor. Higher levels of electric turbochargers were able to reduce the BSFC. The usage of a brushless DC motor on an electric supercharger controller was studied by Bingyong *et al.* [18]. The performance of an electric supercharged engine was improved by getting engine speed and load at various speeds during boosting. Studies on the control systems that may be employed to regulate the energy management of the electric turbocharger system, motor, and battery were also conducted. High-speed synchronous motors were employed by Novák *et al.* [19] to electrically drive the compressors in a turbocharger. High-speed synchronous motor control was used to test electrically powered compressors on overcharged gasoline or diesel engines, and it was discovered that the controls had excellent structure. The battery pack requirements for a mild-hybrid system incorporating an engine with an e-supercharger were researched by Hall *et al.* [20]. It was discovered that a 48V battery pack reduces gasoline usage by between 12 and 15.5 percent throughout a drive cycle. The impact of a 12V or 48V electric supercharger during a driving cycle was studied by Zanelli *et al.* [21]. A 12V electric supercharger was shown to reduce fuel usage by 4% over a range of driving cycles.

Studies on control schemes for the electric turbocharger have been conducted. A system for the characterization, control, and energy management of an electrified turbocharged diesel engine was proposed by Dezong *et al.* [22] in their study. According to this study, an electrified turbocharged diesel engine should have a two-level energy management system that is coherent. In a study to improve the electric power distribution under transient conditions in a hybrid system, Xia *et al.* [23] suggested an electric system architecture. According to the study, using a belt-driven starter generator (BSG) with an electric supercharger improves the engine's fuel efficiency. To calculate the efficiency of the engine when used with a turbo-compound, an analytical model of a 2000 cm3 turbodiesel engine was proposed and validated by Repetto *et al.* [24]. The hybrid system with the supercapacitor and turbo-compound significantly increases engine efficiency, especially at high-load operating points, according to the study. An investigation on the best control methods for high-performance hybrid electric power units was done by Balerna *et al.* [25]. The turbocharger electrification technology, according to the study, increased fuel efficiency by 8%. In a study on a two-stage boosted ultra-lean spark-ignition (SI) engine, Bozza *et al.* [26] offer a calibration methodology with the aim of reducing CO2 emissions. The element that was considered when proposing two calibrated variants of a proportional integral derivative (PID) controller was different fuel and electric consumption. It was discovered that the method that reduced e-compressor consumption resulted in a modest reduction in CO2 emissions. An innovative sensor-less algorithm and variable-frequency drive (VFD) control were studied by Andrew *et al.* [27] to control the energy management of a hybrid-electric turbocharger. The investigation discovered that the VFD performs at an efficiency greater than 98% when operating between 25 and 1050C at full load.

Research involving transient conditions was also reviewed for the objectives of this study. The use of an electric turbocharger to increase the fuel efficiency of long-distance heavy-duty trucks was studied by Ekberg *et al.* [28]. According to the study, an electric turbocharger reduces fuel consumption by 0.9% throughout a drive cycle. Hao *et al.*'s [29] investigation into gasoline vehicle energy management and hybrid turbocharger optimization. The study discovered that the hybrid turbocharger could lessen the turbocharger's associated overcharge issue. Lowering fuel consumption was

made possible by the hybrid turbocharger's ability to reduce pumping losses. According to the study, the fuel-saving potential of an electric turbocharger system varies between 1% and 5% over various driving cycles. The advantages of adding an electric turbo compound to a little twin-cylinder SI engine were assessed by Pasini *et al.* [30]. When an ETC with an adequately sized turbine was operated at different speeds and loads, the fuel consumption decreased by 4%, but there were no gains in terms of fuel consumption for smaller cars operating in urban cycles. When ETC is used, larger cars gain greatly. According to this report, further research must be done on ETC applications such as electric driving.

This research study's evaluation of all prior studies assisted in identifying potential areas for improvement for an electric turbocharger. Due to the rigidity of some electric turbocharger configurations, where the turbine and compressor must be the same size and run at the same speed, it was discovered that energy was still wasted via the wastegate. As a result, the system's ability to recover energy was compromised for the sake of improved transient responsiveness. Out of all the different architectures that were examined, a decoupled electric turbocharging arrangement was found to have the ability to recover energy without affecting the engine's performance. Additionally, the review discovered that most of the investigations were conducted in steady state or generic driving cycles. Realistic data on fuel consumption and the system's capability for energy recovery might be obtained by modeling the decoupled electric turbocharger arrangement using an actual localized driving cycle.

In this study, a 1-D simulation program is used to construct an electric turbocharging system for energy recovery and boosting. In terms of engine performance across a driving cycle, the electric and traditional turbocharging systems are contrasted. A steady state full-load, part-load, and drive cycle will be used to determine the amount of energy that is available for recovery. The engine model utilized for this inquiry and its many configurations are highlighted in the next part, which is followed by the simulation process and outcome analysis.

2.0 METHOD AND MATERIALS

Two engine types with the ability to recover waste heat were used in this study. An electrical turbocharged engine was developed using a 1.6L CamPro CFE engine as its basic model. The CFE engine was chosen because it came from a small passenger car, had a readily available brake torque curve, and had a one-dimensional model that had been verified by Ismail *et al.* [31] when studying the turbocharger marching for residual concentration reduction. The model was found to have an accuracy of 72.6 percent on average across the entire engine speed range and 99 percent between 2000 and 6500 rpm [11]. Table 1 shows the engine specification of the CamPro CFE turbocharged engine.

Table 1. Engine specification of 1.6L CamPro CFE engine [11]

Specification	1.6 liter turbocharged engine
Engine type	4-stroke Spark Ignition
Induction system	Turbocharged
Fuel delivery	Multi-point injection
Compression ratio	9.0
Bore x Stroke (mm)	76 x 86
Capacity (liter)	1.6
Maximum Power @5000 RPM (kW)	103
Maximum Torque @ 2000-4000 RPM (Nm)	205

To regulate the mass flow that travels through the turbine, the turbo engine incorporated a wastegate controller that sensed engine brake mean effective pressure (BMEP). It could rotate at a maximum speed of 200,000 rpm and a maximum diameter of 30mm. This speed restriction is crucial for preventing overspeeding of the turbocharger, which might result in damage to the turbochargers and decreased system performance. Tolerances of 0.05 for engine BMEP, 0.002 for shaft torque imbalance, and 0.002 for average pressure were established in the run setup of the program to achieve a steady state. Once all three of these conditions are satisfied in the simulation, it ends automatically.

The turbo engine model, the CFE engine, was upgraded to include an electronic turbocharger. The motor, wastegate, turboshaft, battery pack, and compressor power demand were the parts and components that required alterations and additions. To fit a generator to the turbine and a motor to the compressor, the turboshaft linking the turbine and the compressor in a standard turbocharger was detached for this experiment. As the output difference between the two engine models was just 0.01 percent, it was determined that the CFE engine was identical to the engine model it was built upon. The 1.6L CamPro CFE electrical turbocharger system with a two-motor setup is shown in Figure 1.

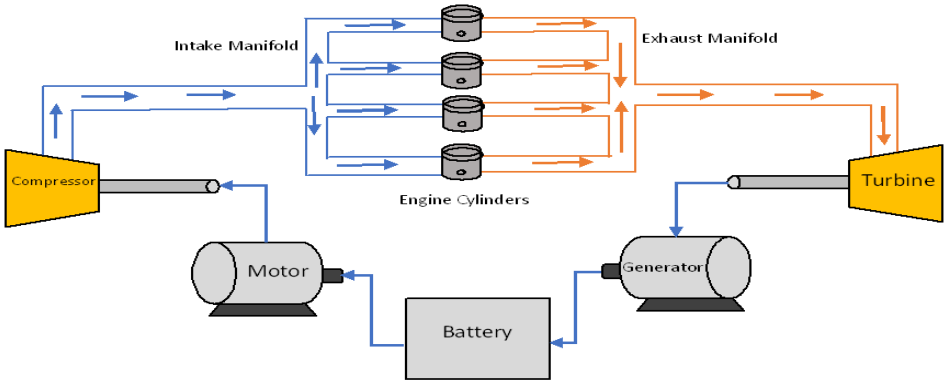

Figure 1. The setup of the electrical turbocharger system

The angular motion equation determined how much power was generated by the motor in relation to the turbine speed since the turbine and the generator were both angularly moving objects. The power produced by the motor (P) is calculated using the equation in Eq. (1) by multiplying the torque (T) and angular velocity (ω) it produces.

$$P = T\,\omega \tag{1}$$

At its top speed of 170,000 rpm, the motor that drives the turbine has a rated power output of 9.6 kW. The compressor's motor's rated power was 11.0 kW, and its maximum rotational speed was 170,000 rpm. 80 percent efficiency was used on both motors to simulate real-world motor performance. The wastegate on the standard model must be recalibrated so that it recognizes the turbine speed and caps its maximum working speed at 170,000 rpm in order to accommodate the two motors. For this study, a 48V battery pack with a 10.5 A-h capacity was adopted. 48V system architecture is seen as the future of the automotive industry based on findings from past studies [20]. Table 2 shows the electrical turbocharged CamPro engine's battery specifications.

Table 2. Battery specification of electrical turbocharged CamPro CFE engine

Specification	Battery
Battery Capacity (A-h)	10.5
Open Circuit Voltage Map, Discharge (V)	48
Open Circuit Voltage Map, Charge	48

When specific requirements are satisfied, the model must attain a steady state to perform a full-throttle simulation. These criteria are configured under the run setup menu, where flow control, ODE control, and heat control form the foundation of the requirements that the model must meet to attain a steady state. One of the boundaries for flow control is the mass flow rate tolerance limit. The boundary for ODE control is the torque imbalance tolerance limit, whereas the thermal solver is set to stable for steady-state simulation and part load simulation, and transient for drive cycle mode.

The automatic shut-off option ensures that the simulation enters a steady state. Automated shut-off may be enabled in the software only for steady-state simulation by entering specific criteria in the run setup where these requirements must converge for automatic activation. RLT convergence in the run setup menu allows users to specify which parameters must converge before the simulation can be completed automatically. The engine BMEP, shaft torque imbalance, and average intake pressure steady-state tolerance were the parameters specified to converge before automated steady-state shut-off in this model.

For part load simulation, the e-turbo engine was tested in eight distinct scenarios, each with a different target torque. The target torques were varying percentages of the maximum brake torque produced by the engine at a steady state, ranging from 12.5% to 100%. All eight cases ran at the same engine speed, which began at 1000 rpm. The model's throttle connection was used to manage the engine load (torque) using a throttle controller. The controller linked to the throttle connector allowed it to manage engine torque by adjusting the throttle angle at the connector. Part load simulations were used to calculate the energy demand from the compressor at various loads and speeds, and the results were used to estimate the compressor power requirement. Figure 2 illustrates how much electrical power the motor supplies to the compressor. A series of part-load simulations was used to produce the power demand map shown in Figure 2 to assess the energy demand of the compressor at various loads and speeds. It was assumed that the speed of the compressor would be equal speed of the motor rotating the compressor when obtaining the data for Figure 2.

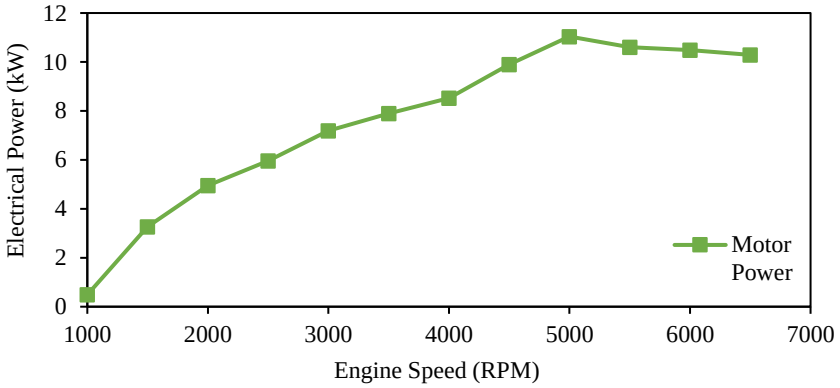

Figure 2. Electrical power from the motor to the compressor

In order to calculate the motor power requirement at various engine speeds and loads, part-load simulation was carried out only on the e-turbo engine model after the steady state simulation was completed. From this simulation, the net energy recovery at various engine speeds and loads was also examined. The e-turbo engine was operated in eight scenarios, each with a distinctive target torque. The targeted torques ranged from 12.5 percent to 100 percent of the brake torque that the engine could deliver at a steady state. These eight cases were all operated at the same engine speed, which was 1000 rpm. The part-load brake torque points at various engine speeds are shown in Figure 3.

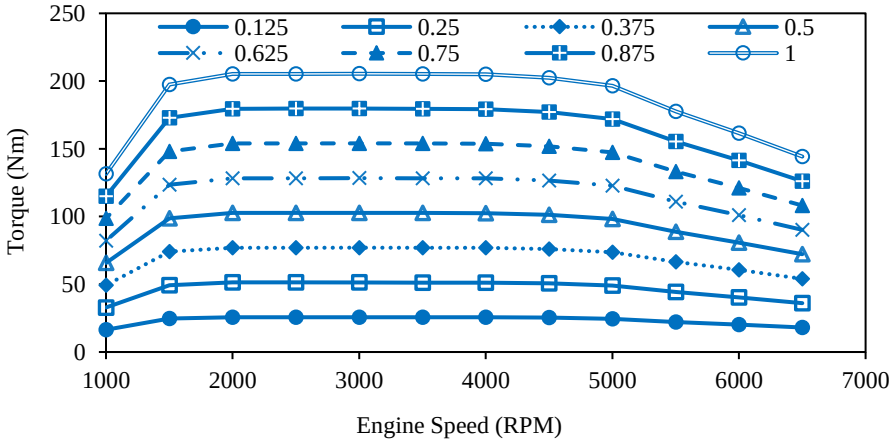

Figure 3. Part-load brake torque points at various engine speeds

The transient analysis of these engines was conducted using an actual driving cycle. The drive cycle was developed using data from actual road testing conducted in the Klang Valley and Kuala Lumpur [32]. The engine speed-torque points of the actual driving cycle are depicted in Figure 4.

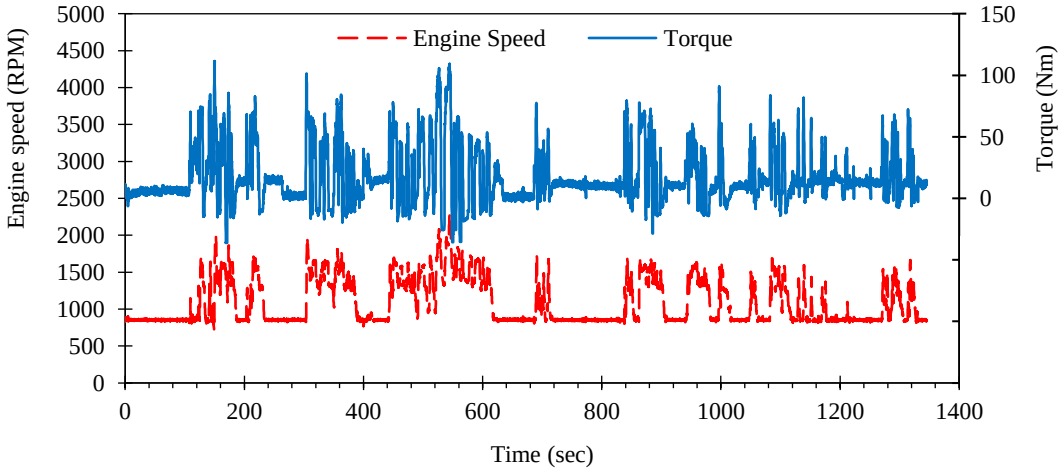

Figure 4. Engine speed-torque points of actual drive cycle [32]

It encompassed a variety of real-world urban driving scenarios, including brief sprints, standstills, and interstate driving, as well as driving patterns with heavy traffic during peak hours. The driving cycle employed in this study lasted 1385 seconds in total, with 100-millisecond intervals between each data point. The number of points that could be used for a single driving cycle simulation was limited by the 1-D simulation program. By splitting the driving cycle into eight portions, the simulation must be run 8 times. Then, for convenience of data analysis, all the information from the eight simulation cycles is combined into a single table.

3.0 RESULTS AND DISCUSSION

The results of the engine simulations for both engines are fully explored. To provide a clear presentation of the findings, the data are shown in figures, graphs, and tables and explained using numerical data and statistics from prior studies. The steady-state and transient analyses for both the turbo CFE engine and the e-turbo CFE engine model are reviewed, while part-load was described for the e-turbo CFE model.

3.1 Steady-State Analysis

The brake power and BMEP output for both engines were identical during the steady-state study. The comparison of the BSFC between the two engine types is shown in Figure 5. The e-turbo engine was found to have a somewhat greater BSFC than the standard engine when at full load. However, at engine speeds between 1000 and 1500 rpm, the e-turbo BSFC outperformed the basic engine. The e-turbo engine's increased exhaust pressure at the exhaust manifold is what led to an increase in BSFC. When researching the usage of an extra turbine in series to the charging turbine of an electric turbocharger, Wei *et al.* [7] also ran into this problem. Wei *et al.* [7] discovered that although energy recovery was achievable over the whole engine range, the engine was hampered by engine pumping losses, which increased back pressure. This idea will be supported by more observations later in the chapter.

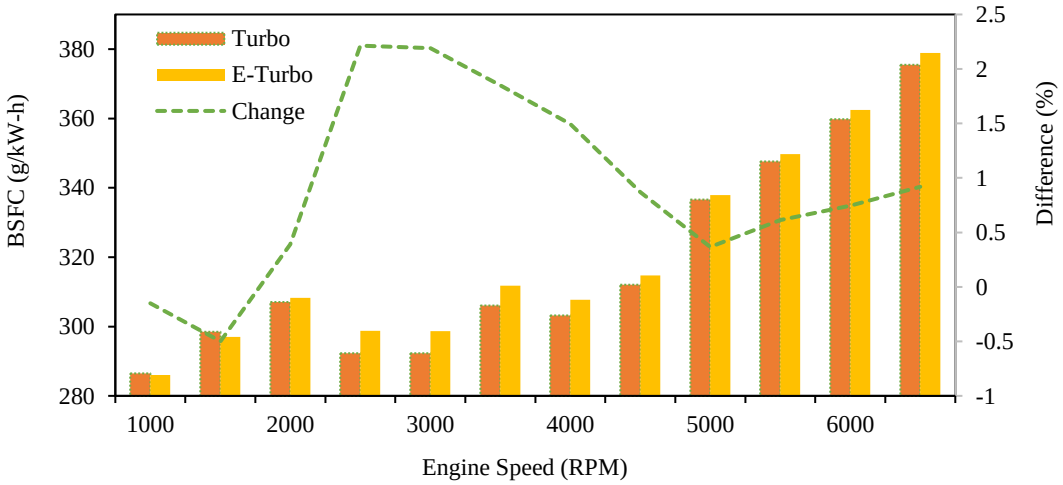

Figure 5. BSFC comparison between turbo engine and e-turbo

Comparing the exhaust pressure from the standard engine with the e-turbo is shown in Figure 6. Over the entire engine speed range, the e-turbo engine's exhaust pressure climbed, with the increase being the most noticeable above 2000 rpm. At 2500 rpm, where the e-turbo engine produced 26.2 percent higher exhaust pressure than its non-electrical version, the difference in exhaust pressure between the two engines was at its greatest. According to the graph's general trend, it was determined that the rise in exhaust pressure and the detected increase in BSFC are related. By countering the increased pressure inside the exhaust manifold, the engine must perform more work to expel the waste exhaust gases into the environment.

As a result, more gasoline was burnt to achieve the same power as the standard CFE engine. Turbine inefficiency restricts airflow, causing the e-turbo engine to produce more exhaust pressure even though energy was created and stored in the battery. Salim *et al.* [2] emphasized this fact while advising that the turbocharged engine utilized to evaluate the advantages of spark-ignition engine fuel-saving technology during transient part load operations be optimized. Turbocharged engines were one of the fuel-saving methods researched. The analysis found that the turbocharger efficiency was less than 50% for the whole driving cycle. The authors advised that an adaptive boosting mechanism be used to fully use the potential of smaller engines.

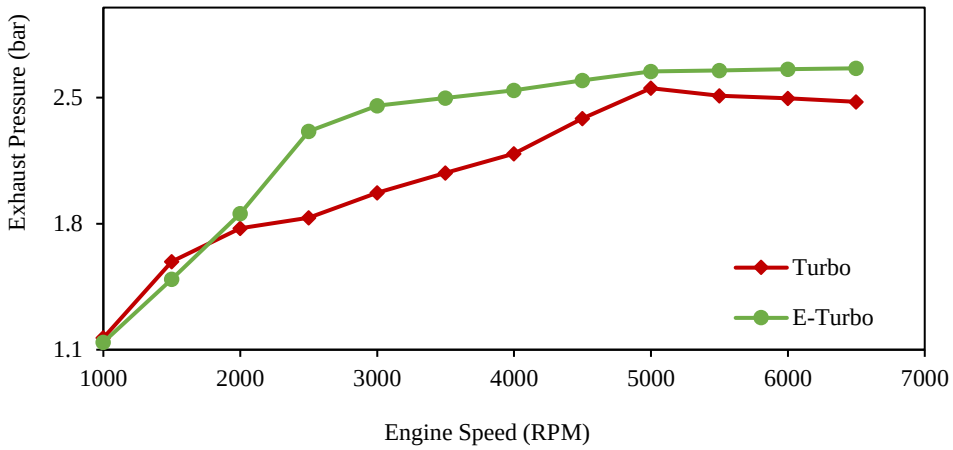

Figure 6. Exhaust pressure comparison between turbo engine and e-turbo

The basic engine (conventional turbocharging) and the e-turbo engine type's turbine speeds are contrasted in Figure 7. The turbine slows down between engine speeds of 1000 and 2000 rpm with an average speed of just 8000 rpm, but after rebounding and exceeding turbo engine speeds at engine speeds of 3000 rpm, it maintains a constant speed of 170,000 rpm. From that point on, the turbine speed is fixed at 170,000 rpm for the whole engine speed range.

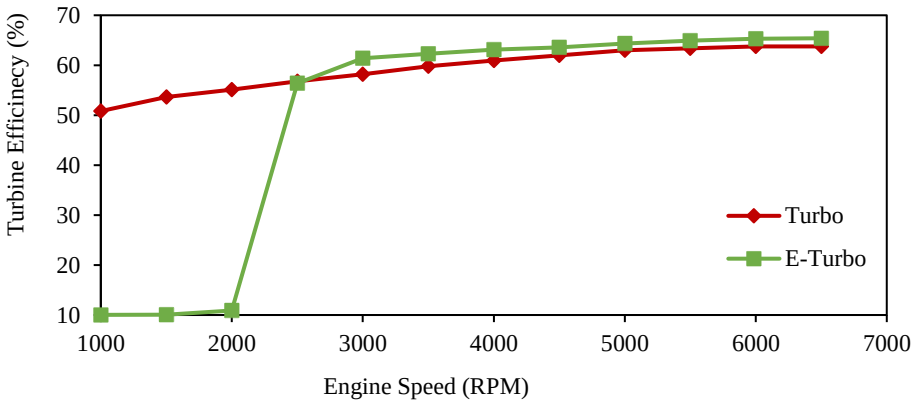

Figure 7. Turbine speed comparison between turbo engine and e-turbo

The installation of two motors and the decoupling of the turboshaft resulted in considerable variation in the dynamics of the turbocharger components. The general trend for the e-turbo turbine speed was that the turbine became inefficient between engine speeds of 1000 to 2000 rpm, with an average speed of only 8000 rpm. The consistent speed of the turbine when the engine hits 3000 rpm highlights the wastegate controller's role in regulating the turbine speed and mass flow rate. This also shows that the generator's motor had reached its maximum working point and would be unable to provide any more electrical power due to the wastegate's limit on turbine mass flow to safeguard the motor. The low turbine speed at low rpm would have resulted in the drivability of the vehicle being sluggish at low speeds. The responsiveness of the engine would improve considerably once it reaches 2500 rpm due to the power produced by the rotating turbochargers. The engine would also struggle in heavy load operation since it would require high torque at very low engine speeds.

When analyzing electric turbo-compounding as a potential method for waste heat recovery for a turbocharged engine, Alias *et al.* [3] noted this motor constraint. It was stated that overheating difficulties at higher motor power levels significantly reduce turbo system efficiency. Overheating happens when the motor's maximum operating speed is exceeded. As a result of these observations, the constraints imposed on the turbine by the motor connection are justified. Because the new motor and turbocharger combination had a significant influence on turbine speeds, as shown in Figure 7, turbine efficiency data needed to be examined to better understand the efficiency points at which the turbine operates for this steady-state simulation.

Figure 8 compares the standard CFE engine with the e-turbo's turbine efficiency. At engine speeds between 1000 and 2000 rpm, the e-turbo engine's efficiency significantly declines in comparison to the turbo engine. The turbines slowed down in this area. This was the region where the turbine was inefficient as seen from Figure 7. Very little energy can be recovered by the generator coupled to the turbine as the efficiency was only 10% at this engine speed range. The gap in turbine efficiency between engine speeds of 2500-6500 rpm drastically decreases as engine speed rises. The gap in turbine efficiency is illustrated in Figure 9 in correspondence to the engine speed.

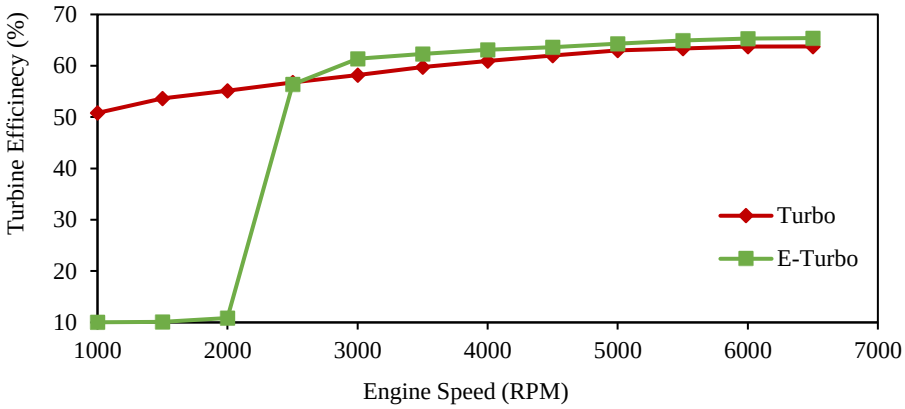

Figure 8. Turbine efficiency comparison between turbo engine and e-turbo

In a turbine map, Figure 9 compares the efficiency operating points of both turbo and e-turbo engine models. It demonstrates the significant variation in turbine efficiency between the two engines at low engine speeds, demonstrating how the turbine map is significantly altered by the inclusion of the generator. The installation of two motors and the decoupling of the turboshaft resulted in considerable variation in the dynamics of the turbocharger components, namely the turbine speed which is closely related to the turbine efficiency as shown in Figure 9. At low engine speeds, the e-turbo engine's turbine functioned at locations outside the zone with the highest efficiency. As a result, there was ineffective energy recovery since the energy in the exhaust gases was not effectively used.

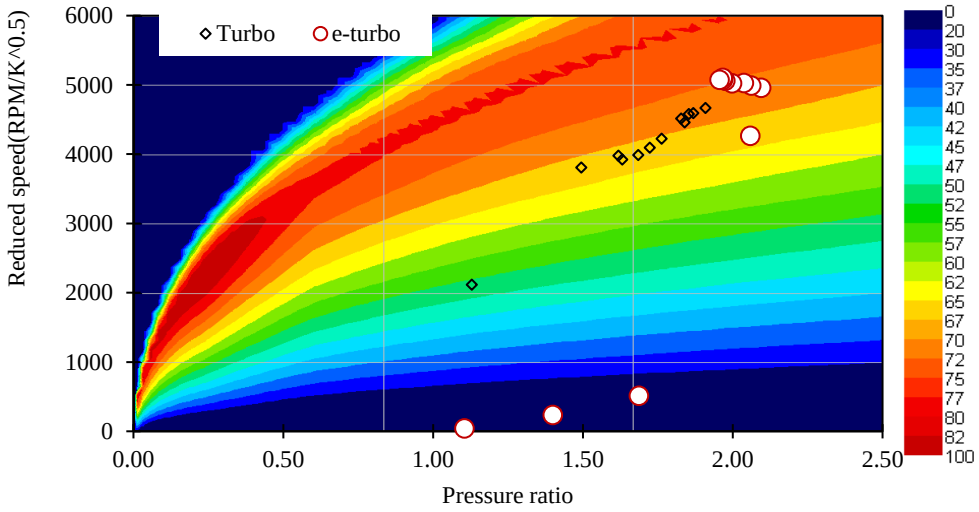

Figure 9. Operating points in a turbine map

The turbine can be optimized to improve the efficiency of the energy recovery process. Optimization based on actual consumer driving habits can boost the potential for energy recovery over the whole engine range. With the decoupled turboshaft arrangement, you may optimize the turbine individually without affecting the transient engine response. Turbine optimization substantially enhances energy recuperation by the generator, since turbine spinning from exhaust gas flow provides electrical power through the generator. When studying waste heat recovery solutions including electric turbo-compounding, Alias *et al.* explored this [3]. The author proposed that high-efficiency turbine wheels be utilized to minimize back pressure and, as a result, the engine's fuel consumption.

The compressor speed comparison between the standard engine and the e-turbo engine is shown in Figure 10. The difference between the two engines' compressor speeds was practically identical at low engine speeds of 1000–2000 rpm. The difference in speed was only noticeable above 2500 rpm, with the largest difference between the two engines occurring at 3000 rpm when the electric turbocharged engine was working more quickly than the turbo engine.

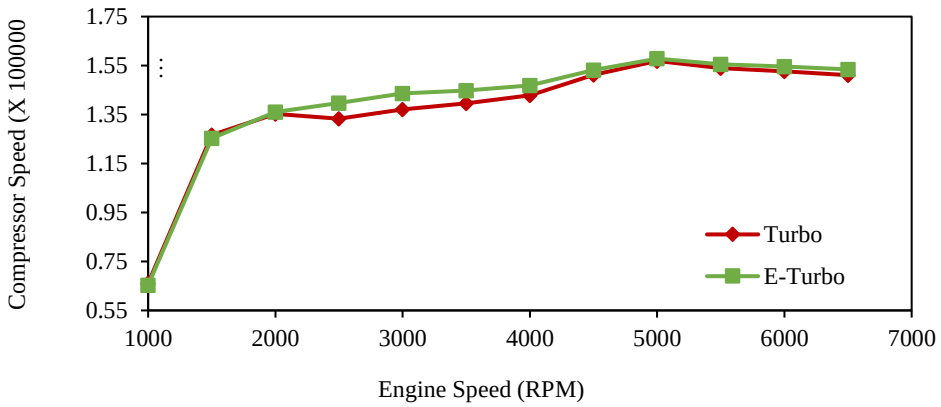

Figure 10. Compressor speed comparison between turbo engine and e-turbo

The wastegate valve diameter comparison between the turbo engine and the e-turbo engine is shown in Figure 11. The wastegate valve of the e-turbo engine was completely closed at engine speeds between 1000 and 2500 rpm, enabling all the exhaust gases to travel through the turbine. Up to 5000 rpm, the difference in wastegate diameter increased further with increasing engine speed, at which time the valve opening widths were identical. Since the primary goal of this research was to convert exhaust gases into electrical energy. As a result, the e-turbo's wastegate was designed to enable more mass flow into the turbine, given that the compressor was now a separate free-body entity with its own controls for regulating boost pressure. The wastegate valves of the e-turbo engine were designed to open narrower to enable more exhaust gases to travel through the turbine and allow the generator attached to the turbine to create electrical energy from the turbine's spin.

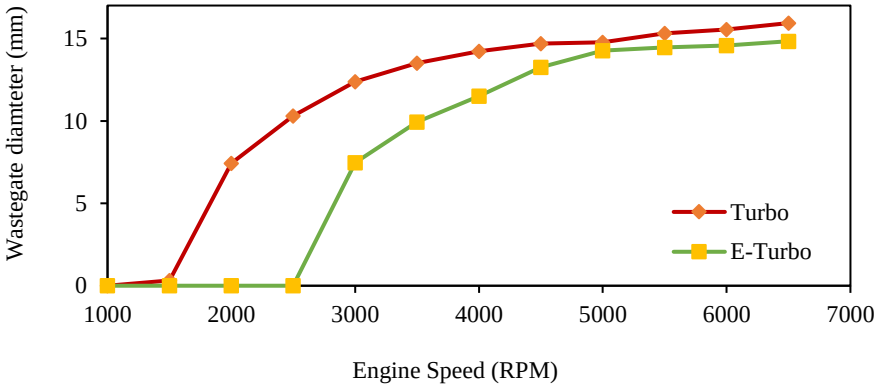

Figure 11. Wastegate diameter comparison between turbo engine and e-turbo

The net electrical energy recovery by the electric turbocharging system is shown in Figure 12. The net energy recovery was only positive in two zones. The net energy recovery was 0.57 kW at 2500 rpm and 0.5 kW at 3000 rpm, respectively. The positive net energy recovery is possible between 2500 to 3000 due to the wastegate allowing a higher mass flow rate through the turbine compared to the conventional turbo. The new control mechanism for the wastegate allows for the mass flow rate of the turbine to be higher, thus allowing more energy to be recuperated by the generator. All the remaining engine speed values, which ranged from 1000 to 2500 rpm and 3000 to 6500 rpm, had negative net energy recovery.

Based on these results, the motor spent more electrical energy to meet the torque demand indicated by the throttle controller, however, no energy was recovered or consumed when the engine was idle. While this drive cycle had relatively low engine speeds and loads, a new drive cycle with somewhat higher engine speeds might be able to demonstrate the decoupled electric turbocharger setup's energy recovery capacity.

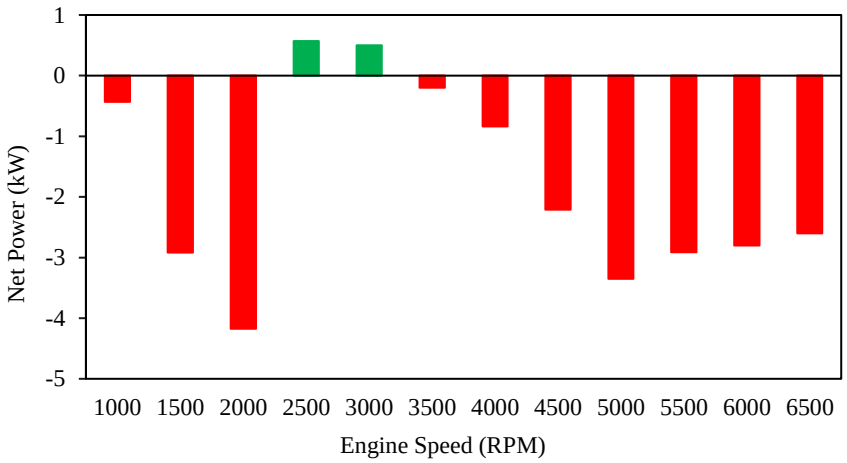

Figure 12. Net energy recovery at different engine speeds

3.2 Part-Load Analysis

The analysis for part load simulation concentrated on the energy recovery of the e-turbo. Figure 13 shows the net energy recovery. At engine rpm of 1000 to 2000, there was no positive energy recovery. At 0.28 kW at 5000 rpm, or 37.5 percent engine load, the net energy recovery was positive at the lowest engine load point. At full throttle, the engine's lowest operating speed where surplus energy could be recovered was 2500 rpm (100 %). The engine was running at 37.5 percent load when the greatest electrical energy was recovered, 5.25 kW, was recovered at 6500 rpm. The least amount of energy was likewise recovered at 5000 rpm, 0.28 kW. The lowest engine load point at which the net energy recovery was positive was 0.28 kW at 5000 rpm, 37.5% engine load. It can be observed that energy recovery was possible at low engine speeds of this e-turbo engine model because energy was recovered at 2500 rpm. Nevertheless, it was apparent that the energy recovery was more prominent at medium to high engine speeds as energy was recovered at a low engine load of 37.5 % at high engine speeds.

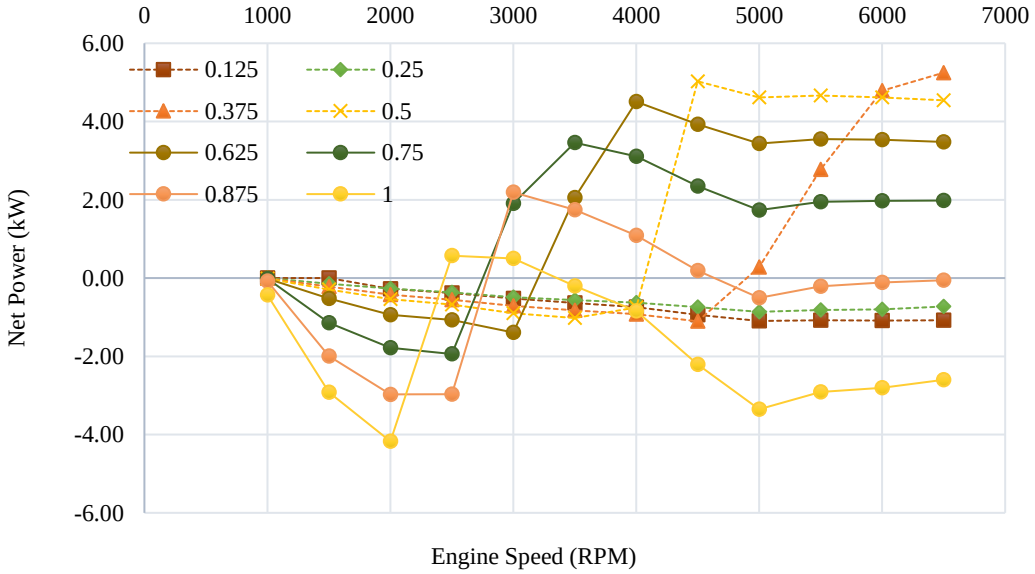

Figure 13. Net energy recovered at different engine loads

3.3 Drive Cycle Analysis

Numerous evaluations were conducted for the transient condition based on an actual driving cycle. The contrast between the e-turbo engine's speed-load points and full-load torque production is shown in Figure 14 of the driving cycle. In a driving cycle simulation, the torque output of the basic engine and the e-turbo engine differed by 0.3 percent on average. The minor difference in torque produced by both engines demonstrated that both engines had the same torque performance, reaffirming the steady state and part-load brake torque statistics. The similar torque output of both engines in a drive cycle was important because no changes were made to the turbine and compressor maps, as this would have deviated from the focus of this study, which was to investigate the energy recovery potential of an electrically turbocharged CFE engine and its impact on fuel consumption in an actual drive cycle. The steady-state and part-load brake torque measurements are confirmed by the same torque performance of both engines. Figure 15 shows that throughout the entire driving cycle, the engine worked at low speed and low load areas. The driving cycle's torque points were all far below the e-turbo engine's maximum torque output. The engine's average brake torque for the drive cycle was

just 40 Nm, or 30% of its lowest torque output at full speed. It can be seen that most of the power demand points were concentrated at low engine speeds and low power demand. Since this drive cycle is ultra-urban, this explains the reason why the drive cycle was of very low engine speeds and loads.

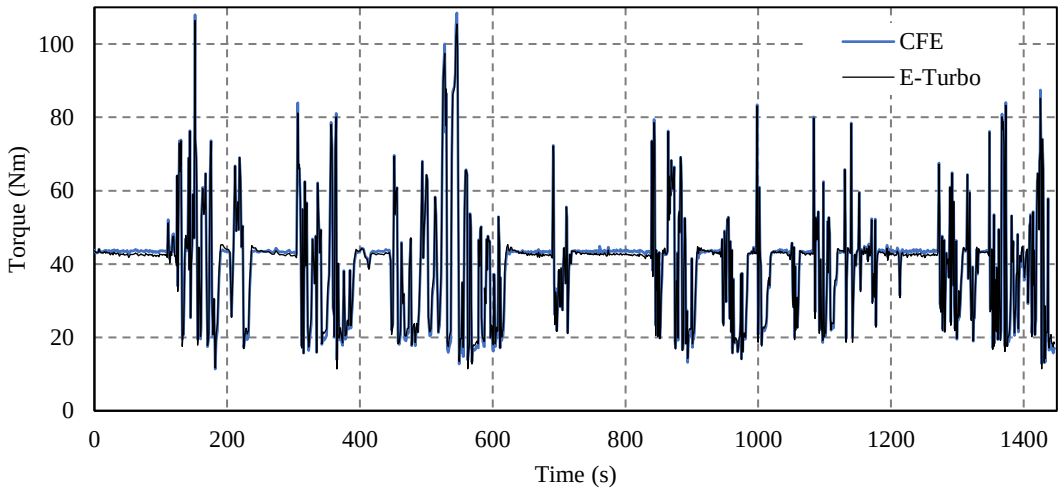

Figure 14. Brake Torque comparison between turbo engine and e-turbo in the drive cycle

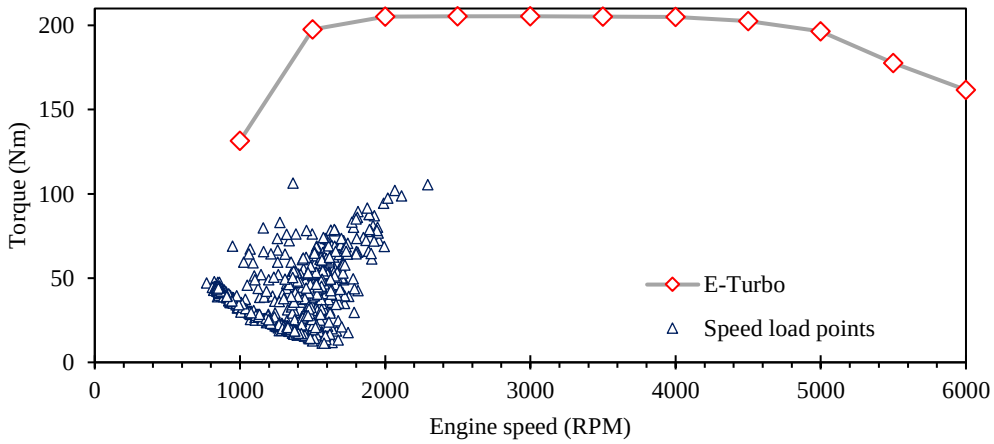

Figure 15. Speed-load points of drive cycle on a full throttle torque output curve of e-turbo engine

Figure 16 compares the torque profile of the driving cycle with the fuel mass flow rate for the standard CFE engine and the e-turbo engine. Since there was only a 0.05 percent difference between the two engine types, it can be assumed that the fuel mass flow rate during the whole drive cycle was similar. Throughout the entire driving cycle, both engines exhibited an average fuel mass flow rate of 0.55 g/s. The average fuel mass flow rate between these parts of the driving cycle was 0.74 g/s for both engines. This was 34.5 percent greater than the total average fuel mass flow rate. The significant spikes in torque demand that can be seen in the torque demand profile were the cause of the higher-than-average fuel mass flow rate, especially because the driving cycle's peak torque demand was reached during this time. At high torque demand, the turbo engine has a larger fuel flow rate than the e-turbo engine type, although it was lower than the e-turbo at low torque demand. This was confirmed in the results of prior research on hybrid turbocharger analysis in motor vehicles driven by internal combustion engines by Jovan *et al.* [5]. According to the study, a rise in fuel mass flow rate and an increase in engine speed were related. The author also claimed that engine performance barometers like volumetric efficiency and in-cylinder temperature have an impact on fuel mass flow rate. The study also discovered that using hybrid turbochargers results in higher engine efficiency by 10-12%.

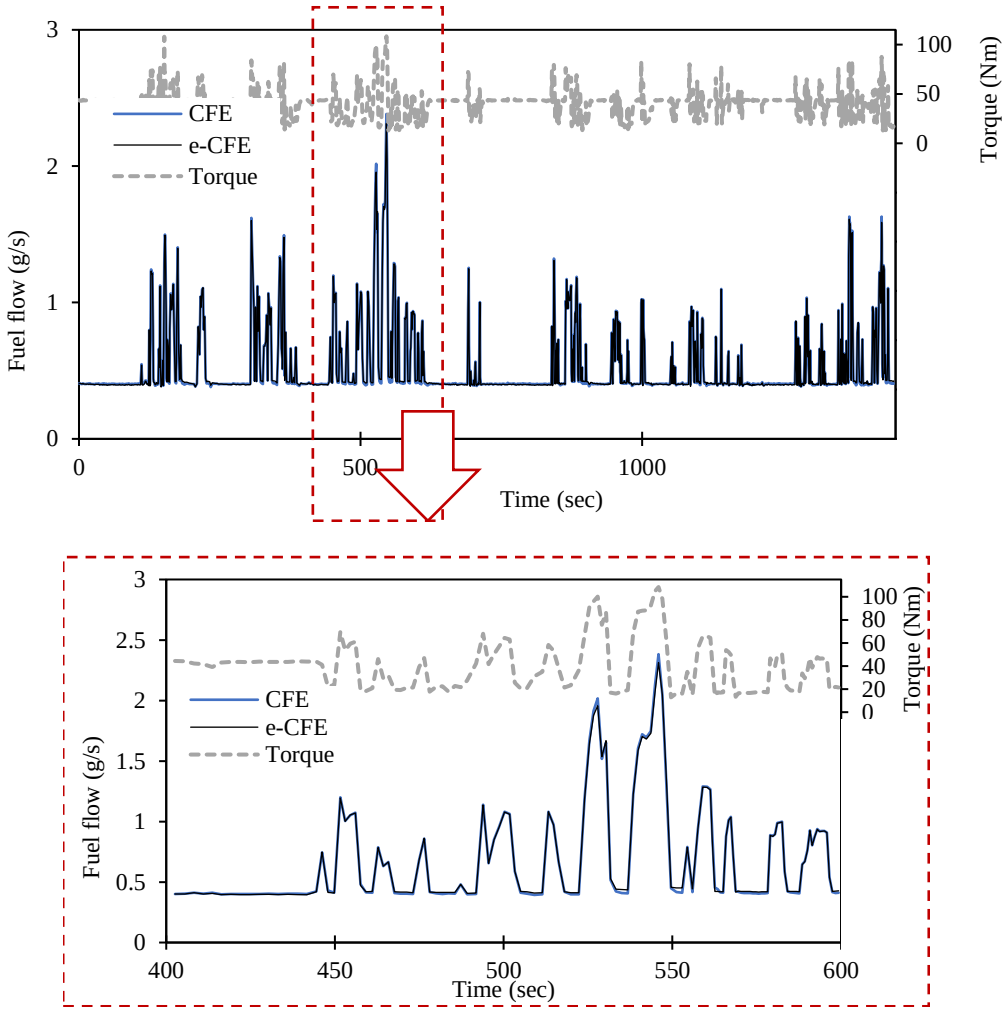

Figure 16. Fuel mass flow rate comparison between turbo engine and e-turbo in drive cycle with torque demand profile

A comparison of the total fuel consumption of the two engines over a driving cycle with the engine speed profile is shown in Figure 17. Over the course of the driving cycle, the standard CFE engine with a traditional turbocharger arrangement used 753.2 grams of gasoline, compared to 752.2 grams for the e-turbo engine with two electric motors. Due to the extremely modest percentage of fuel savings, both engines had the same fuel consumption. The e-turbo engine's exhaust pressure was found to be slightly lower, but it was not enough of a difference to affect fuel consumption. Numerous variables may be responsible for the same fuel consumption of the two engines. The wastegate controller's calibration somewhat decreased. The installation of two electric motors penalizes the otherwise higher back pressure.

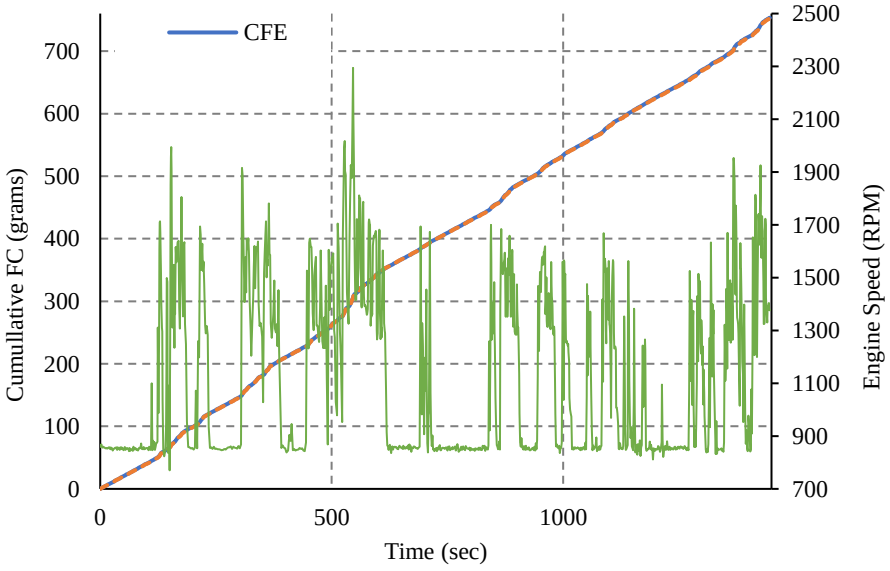

Figure 17. Cumulative fuel consumption comparison for CFE and e-turbo engine

Figure 18 depicts a compressor map with the e-operating turbo's locations. The compressor functioned within a relatively narrow operational zone, as can be seen in the figure. Low mass flow rate and pressure ratios were present in this area of the compressor map. Between 30 and 60 percent of the compressor map's efficiency was in this area. Throughout the whole driving cycle, the compressor worked with an average efficiency of 37.9%. The CFE engine and the e-turbo engine were not optimized for this driving cycle, as can be seen from these statistics and graphs. Therefore, this was the cause of the compressor's low efficiency. However, the adaptable electric turbocharger configuration for the e-turbo engine allows for a boosting system where the compressor and turbine diameters may vary. Salim *et al.* [2] proposed the necessity for an adaptive boosting technology to address the drawbacks of the traditional turbocharger. According to the study's recommendations, the turbocharger should be further optimized to lower fuel usage throughout the drive cycle. A smaller turbocharger would enable it to work in areas of the compressor map that are considerably more efficient but would significantly lower the engine's maximum output.

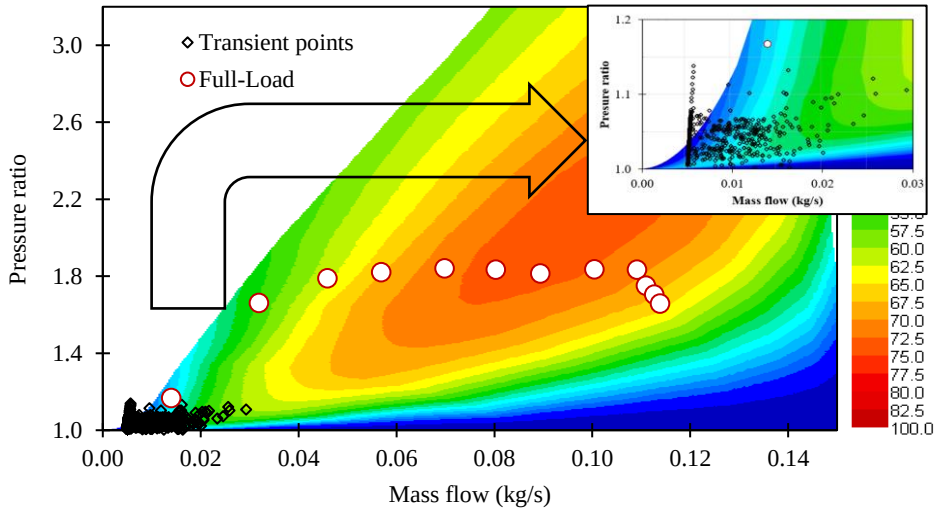

Figure 18. Full-load and drive cycle operating points on e-turbo compressor map

Figure 19 displays the torque profile of the driving cycle together with the net electrical energy recovery of the e-turbo engine type. It is obvious that the motor used more electrical energy to meet the torque requirement set by the throttle controller, but no energy was recovered or used when the engine was idle. Figure 20 depicts the motor's electrical power points throughout the transient simulation as well as the power requirement at maximum throttle. Most of the engine's power demand points were located at low engine speeds. Additionally, the motor power points were located between 2500 and 3000 rpm, right before the e-energy turbo's recovery area.

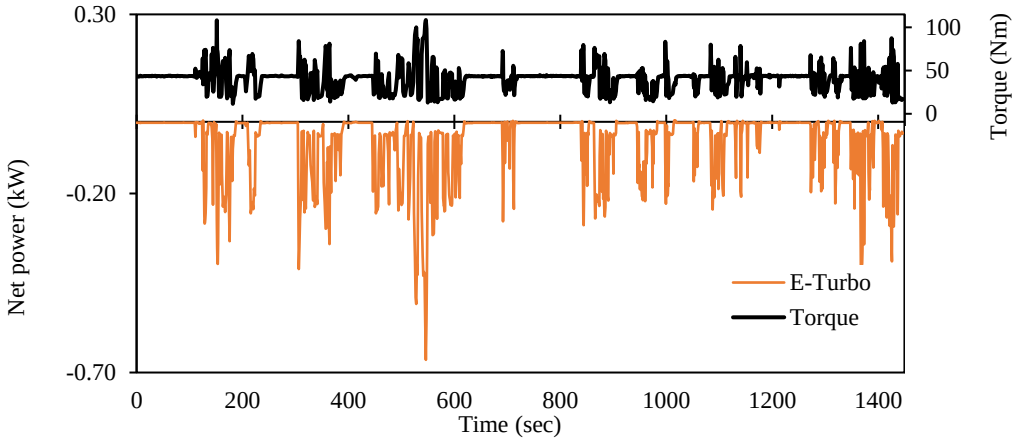

Figure 19. Net electrical energy recovery of e-turbo in drive cycle with torque demand profile

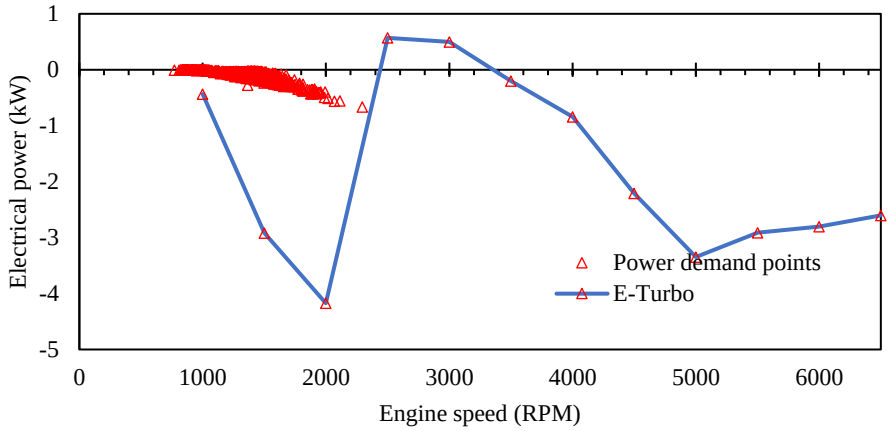

Figure 20. Electrical power points throughout the transient simulation and steady state power demand of the motor

4.0 CONCLUSIONS

To simulate an electrical turbocharged engine and forecast its performance throughout a real driving cycle, simulation-based research was conducted. Three stages made up the simulation process. The standard engine model and the electrical turbocharged engine were both driven at full throttle during the steady-state full load simulation to calculate the maximum brake torque (Nm) and brake power (hp). The electrical turbocharged engine was next subjected to part-load simulation, in which the engine model was made to run at a constant engine speed but with variable engine torque loads. By increasing the engine speed, the simulation was repeated. Finally, a transient simulation based on an actual driving cycle was used to operate both the basic engine and the electrical turbocharged engine. Net electrical energy recovery was the main piece of information gathered to examine the energy recovery capability and impacts of the electric boosting system on engine performance (kW). The engine's BSFC (g/kW-h) was calculated using steady-state full and steady-state portion loads. For the fuel economy for transient simulation, the cumulative fuel consumption was noted. The following conclusions may be drawn from the simulation data and the analysis that was done on it: -

a) The decoupled turbocharger configuration employed in this study was capable of boosting energy recovery systems. The electrical turbocharger system's ability for energy recovery was proved by the 0.57 kW energy recovered at 2500 rpm in a steady-state. At maximum load, the boost pressure generated by the e-turbo engine and the turbo engine were equivalent, with the e-turbo engine producing about 0.68% less boost pressure. The e-turbo engine was able to equal the standard CFE engine's maximum performance output thanks to the electric turbocharger's adequate boosting, as the brake torque and brake power curves had identical outputs with an average difference of just 0.01% for both engines.

b) At steady state conditions, it was discovered that the e-turbo BSFC increased the most at 2500 rpm by 2.2% before the rate of increase started to decrease to 0.37% at 5000 rpm, while the increase rate was the lowest at 2000 rpm for the e-turbo at 0.39%. The BSFC decreases slightly at engine speeds of 1000 rpm and 1500 rpm by 0.15% and 0.5% respectively. The cumulative fuel consumption difference between the two engines amounts to a 0.05% reduction in fuel consumption under transient circumstances involving a real drive cycle. Despite this, due to the extremely modest percentage of fuel-saving, both engines had the same fuel consumption.

c) Only between steady-state full-throttle engine speeds of 2500 rpm and 3000 rpm was energy recovery feasible. At steady state circumstances, 0.57 kW and 0.5 kW of energy were recovered, respectively. From the part-load simulation results, electrical energy recovery at various engine loads and speeds was acquired. Energy recovery at the lowest engine load point was 0.28 kW at 5000 rpm or 37.5% engine load.

The following suggestions should be considered while conducting more studies on this electrical turbocharger configuration:

- The best turbine and compressor size for this configuration may be determined by conducting a turbocharger matching study.
- To increase the total engine performance output and fuel consumption, research may be done on the best-boosting performance.
- To enhance the power delivery and energy storage of an electrical turbocharger configuration, more research on various control techniques might be conducted.
- The validation of data obtained from this study can be done by designing and fabricating an electrical turbocharger like the simulation model where the original turbocharger was decoupled to fit the motor and carrying out drive cycle and dyno test to obtain its fuel consumption and brake torque and power data respectively.

5.0 ACKNOWLEDGEMENT

This work was supported by Universiti Tun Hussein Onn Malaysia (UTHM) (RE-GG)-Q206.

6.0 REFERENCES

[1] European Parliament and Council of the European Union, "Regulation (EC) No 715/2007 of the European Parliament and of the Council of 20 June 2007 on type approval of motor vehicles with respect to emissions from light passenger and commercial vehicles (Euro 5 and Euro 6) and on access to vehicle repair and maintenance information," *Official Journal of the European Union*, vol. L171, pp. 1–16, 2007.

[2] W. S. I. W. Salim, A. A. M. Mahdi, M. I. Ismail, M. A. Abas, R. F. Martinez-Botas, and S. Rajoo, "Benefits of spark-ignition engine fuel-saving technologies under transient part load operations," *Journal of Mechanical Engineering and Sciences*, vol. 11, no. 4, pp. 2289–4659, 2017.

[3] A. M. Noor, R. C. Puteh, and S. Rajoo, "Waste heat recovery technologies in turbocharged automotive engine – A review," *Journal of Modern Science and Technology*, vol. 2, no. 1, pp. 108–119, 2014.

[4] D. E. Winterbone, R. S. Benson, A. G. Mortimer, P. Kenyon, and A. Stotter, "Transient response of turbocharged diesel engines," *SAE Technical Papers, SAE International*, vol. 86, no.1, pp. 465-490, Feb. 1977.

[5] I. Grujic and N. Nikolic, "Analysis of hybrid turbocharger in motor vehicle Ic engine," International Congress Motor Vehicle & Motors 2018, Kragujevac, Serbia, 2018.

[6] N. A. Khripach, L. Y. Lezhnev, A. P. Tatarnikov, et al., "Turbo-generators in energy," *Journal of Mechanical Engineering*, vol. 14, no. 3 pp. 1009-1018, 2018.

[7] W. Wei, W. Zhuge, Y. Zhang, and Y. He, "Comparative study on electric turbo-compounding systems for gasoline engine exhaust energy recovery," *Proceedings of the ASME Turbo Expo*, vol. 5, no. October, pp. 531–539, 2010.

[8] W. Lee, E. Schubert, Y. Li, S. Li, D. Bobba, and B. Sarlioglu, "Electrification of turbocharger and supercharger for downsized internal combustion engines and hybrid electric vehicles-benefits and challenges," *2016 IEEE Transportation Electrification Conference and Expo, ITEC 2016*, 2016.

[9] D. V. Pinto, C. R. Altafini, D. A. Gonçalves, and G. D. Telli, "Comparative analysis of vehicle turbochargers in energy microgeneration for different compoundings," *Journal of the Brazilian Society of Mechanical Sciences and Engineering*, vol. 43, no. 1, p. 14, 2021.

[10] M. Alshammari, F. Alshammari, and A. Pesyridis, "Electric boosting and energy recovery systems for engine downsizing," *Energies (Basel)*, vol. 12, no. 24, p. 4636, 2019.

[11] M. H. M. Muhammad, A. M. I. Mamat, and W. S. W. Salim, "Exergy Analysis of Organic Rankine Cycle and Electric Turbo Compounding for Waste Heat Recovery," *International Journal of Engineering & Technology*, vol. 7, no. 3.11, p. 152, 2018.

[12] M. S. Imran and H. J. Kurji, "Waste heat conversion in compression ignition engine to the electric power by using exhaust heat recovery system contained TEG," *Journal of Mechanical Engineering Research and Developments*, vol. 42, no. 5, pp. 101–105, 2019.

[13] P. Dimitriou, R. Burke, Q. Zhang, C. Copeland, and H. Stoffels, "Electric turbocharging for energy regeneration and increased efficiency at real driving conditions," *Applied Sciences (Switzerland)*, vol. 7, no. 4, p. 350, 2017.

[14] X. Liu, A. Srna, Q. N. Chan, and S. Kook, "Effect of Exhaust Gas Recirculation and Intake Air E-Boosting on Gasoline Compression Ignition Combustion," *SAE International Journal of Engines*, vol. 13, no. 3, pp. 377–390, 2020.

[15] A. Gilson, R. Sindjui, B. Chareyron, and M. Milosavljevic, "No-load loss separation of high-speed electric motors for electrically-assisted turbochargers," *Proceedings - 2020 International Conference on Electrical Machines, ICEM 2020*, pp. 2439–2444, 2020.

[16] A. El-Shahat, A. Hunter, M. Rahman, and Y. Wu, "Ultra-high speed switched reluctance motor-generator for turbocharger applications," *Energy Procedia*, vol. 162, pp. 359–368, 2019.

[17] M. Alshammari, N. Xypolitas, and A. Pesyridis, "Modelling of electrically-assisted turbocharger compressor performance," *Energies (Basel)*, vol. 12, no. 6, p. 975, 2019.

[18] B. Gou, Y. Yang, and H. Guo, "Design on electric supercharger controller based on Brushless DC motor," *2015 International Power, Electronics and Materials Engineering Conference*, Atlantis Press, pp. 764–767, 2015.

[19] L. Novák, J. Novák, and M. Novák, "Electrically-driven compressors on turbocharged engines with high-speed synchronous motors," *2009 8th International Symposium on Advanced Electromechanical Motion Systems and Electric Drives Joint Symposium*, Lillie, France, pp. 1-6, 2009.

[20] J. Hall, S. Borman, B. Hibberd, et al., "48 v high-power battery pack for mild-hybrid electric powertrains," In: J. Liebl, (eds) Der Antrieb von morgen 2020 Proceedings. Springer Vieweg, Wiesbaden, 2020.

[21] A. Zanelli, F. Millo, and M. Barbolini, "Driving cycle and elasticity manoeuvres simulation of a small SUV featuring an electrically boosted 1.0 L gasoline engine," *SAE Technical Papers*, no. 2019-24-0070, pp. 551–566, 2019.

[22] D. Zhao, E. Winward, Z. Yang, R. Stobart, and T. Steffen, "Characterisation, control, and energy management of electrified turbocharged diesel engines," *Energy Convers Manag*, vol. 135, pp. 416–433, 2017.

[23] F. Xia, P. Griefnow, F. Tidau, M. Jakoby, S. Klein, and J. Andert, "Electric torque assist and supercharging of a downsized gasoline engine in a 48V mild hybrid powertrain," *Proceedings of the Institution of Mechanical Engineers, Part D: Journal of Automobile Engineering*, vol. 235, no. 5, pp. 1245–1255, 2021.

[24] M. Repetto, M. Passalacqua, L. Vaccaro, M. Marchesoni, and A. P. Prato, "Turbocompound power unit modelling for a supercapacitor-based series hybrid vehicle application," *Energies (Basel)*, vol. 13, no. 2, p. 447, 2020.

[25] C. Balerna, N. Lanzetti, M. Salazar, A. Cerofolini, and C. Onder, "Optimal low-level control strategies for a high-performance hybrid electric power unit," *Applied Energy*, vol. 276, p. 115248, 2020.

[26] F. Bozza, V. De Bellis, E. Malfi, L. Teodosio, and D. Tufano, "Optimal calibration strategy of a hybrid electric vehicle equipped with an ultra-lean pre-chamber SI engine for the minimization of CO2 and pollutant emissions," *Energies (Basel)*, vol. 13, no. 15, p. 4008, 2020.

[27] A. L. Carpenter, T. L. Beechner, B. E. Tews, and P. E. Yelvington, "Hybrid-electric turbocharger and high-speed SiC variable-frequency drive using sensorless control algorithm," *Journal of Engineering for Gas Turbines and Power*, vol. 140, no. 12, pp. p.122801, 2018.

[28] K. Ekberg and L. Eriksson, "Improving fuel economy and acceleration by electric turbocharger control for heavy duty long haulage," *IFAC-PapersOnLine*, vol. 50, no. 1, pp. 11052–11057, 2017.

[29] H. Dong, Z. Zhau, J. Fu *et al.*, "Experiment and simulation investigation on energy management of a gasoline vehicle and hybrid turbocharger optimization based on equivalent consumption minimization strategy," *Energy Conversion and Management*, vol. 226, p. 113518, 2020.

[30] G. Pasini, G. Lutzemberger, S. Frigo *et al.*, "Evaluation of an electric turbo compound system for SI engines: A numerical approach," *Applied Energy*, vol. 162, pp. 527–540, 2016.

[31] I. Ismail, A. Costall, M.-B. Ricardo, and S. Rajoo, "Turbocharger matching method for reducing residual concentration in a turbocharged gasoline engine," *SAE Technical Papers*, no. 2015-01-1278, pp. 1-10, 2015.

[32] M. A. Abas, W. S. Wan Salim, M. I. Ismail, S. Rajoo, and R. Martinez-Botas, "Fuel consumption evaluation of SI engine using start-stop technology," *Journal of Mechanical Engineering and Sciences*, vol. 11, no. 4, pp. 2967–2978, 2017.